J. Phys.: Condens. Matter **12** (2000) 3267–3280. Printed in the UK PII: S0953-8984(00)10321-2

An x-ray diffraction and Raman spectroscopy investigation of A-site substituted perovskite compounds: the $(Na_{1-x}K_x)_{0.5}Bi_{0.5}TiO_3$ ($0 \leqslant x \leqslant 1$) solid solution

J Kreisel†‖, A M Glazer†, G Jones‡, P A Thomas‡, L Abello§ and G Lucazeau§

† Clarendon Laboratory, University of Oxford, Parks Road, Oxford OX1 3PU, UK
‡ Department of Physics, University of Warwick, Coventry CV4 7AL, UK
§ Laboratoire d'Electrochimie et de Physicochimie des Matériaux et des Interfaces, ENSEEG, BP 75, 38402 St Martin d'Hères Cédex, France

E-mail: kreisel@physics.ox.ac.uk

Received 13 November 1999, in final form 15 February 2000

Abstract. The $(Na_{1-x}K_x)_{0.5}Bi_{0.5}TiO_3$ perovskite solid solution is investigated using x-ray diffraction (XRD) and Raman spectroscopy in order to follow the structural evolution between the end members $Na_{0.5}Bi_{0.5}TiO_3$ (rhombohedral at 300 K) and $K_{0.5}Bi_{0.5}TiO_3$ (tetragonal at 300 K). The Raman spectra are analysed with special regard to the hard modes and suggest the existence of nano-sized $Bi^{3+}TiO_3$ and $(Na_{1-2x}K_{2x})^{+}TiO_3$ clusters. The complementary use of XRD and Raman spectroscopy suggests, in contrast to previous reported results, that the rhombohedral $\leftrightarrow$ tetragonal phase transition goes through an intermediate phase, located at $0.5 \leqslant x \leqslant 0.80$. The structural character of the intermediate phase is discussed in the light of sub- and super-group relations.

1. Introduction

In the past, structural phase transitions (SPTs) have been extensively studied, with ABO_3 perovskite type structures being one of the largest classes of materials investigated. The particular interest in perovskite solid solutions is twofold. From a fundamental point of view, perovskite solid solutions are attractive since their extensive range of structural variations leads to a detailed understanding of solid solutions and their related phase transitions. From an application point of view, the study of changes of phases in perovskite solid solutions is considered to be important, because solid solutions with a composition close to an SPT are known to present interesting physical properties. One of the best known examples is the technologically important $Pb(Zr_xTi_{1-x})O_3$ (PZT) near the so called morphotropic phase boundary [1].

It is well known that most perovskites can form solid solutions and compounds by altering the composition of the B site of the perovskite structure. On the other hand, there is only a handful of cases of compound formation resulting from the substitution at the A sites, i.e. a chemical formula having its constituents in fixed stoichiometric ratios. $Na_{0.5}Bi_{0.5}TiO_3$ (NBT) and $K_{0.5}Bi_{0.5}TiO_3$ (KBT) are two of these rare perovskites and, therefore, occupy an important niche in the wide field of perovskite structural science.

‖ Corresponding author.

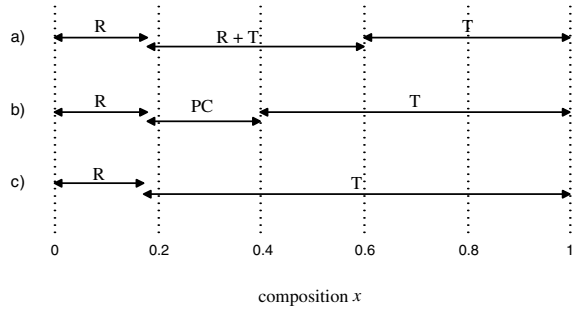

Figure 1. $(Na_{1-x}K_x)_{0.5}Bi_{0.5}TiO_3$ crystal structures (R: rhombohedral, T: tetragonal, PC: pseudo-cubic) as reported in the literature; (a) [3], (b) [2], (c) [4].

In the past years, NBT-related solid solutions like $(Na_{1-x}K_x)_{0.5}Bi_{0.5}TiO_3$ [2–4], $(Na_{0.5}Bi_{0.5})_{1-x}Pb_xTiO_3$ [5–9] or $(Na_{0.5}Bi_{0.5})_{1-x}Sr_xTiO_3$ [10–12] have attracted interest, mainly because of potentially interesting electromechanical properties at the structural phase boundary between the two end members. NBT on its own is known to be a relaxor ferroelectric [13, 14]. The phases in NBT-related solid solutions have been studied by x-ray diffraction (XRD), which gives information about long-range order. Raman spectroscopy, on the other hand, is known to be an appropriate technique for the investigation of the short-range order [15–18] and phase transitions in perovskites [17–20]. To the best of our knowledge, Raman spectroscopy has never been used for the study of NBT-related solid solutions, whereas Raman reference spectra of pure NBT can be found in the literature [21–23].

The $(Na_{1-x}K_x)_{0.5}Bi_{0.5}TiO_3$ (NKBT) solid solution has two particular features: firstly, the above-mentioned compound formation and, secondly, the most commonly studied relaxor ferroelectrics have pairs of chemically different but isovalent B^{4+} cations, whereas NKBT has unlike-valency Na^+/K^+ and Bi^{3+} cations in A positions. These different and interesting features form the basis of this study.

Although NKBT has already been studied by x-ray diffraction and dielectric/piezoelectric measurements [2–4], one can observe discrepancies in the literature on the nature of the $Na_{0.5}Bi_{0.5}TiO_3$ (rhombohedral) to $K_{0.5}Bi_{0.5}TiO_3$ (tetragonal) phase transition. As shown in figure 1, the controversy concerns mainly the $0.16 \leqslant x \leqslant 0.6$ region, where the phase boundary is assumed to be located. The objective of this study is the complementary use of XRD and Raman spectroscopy for the reinvestigation of the room-temperature phase in NKBT.

2. Experiment

Crystals of the NKBT solid solution were grown via spontaneous flux crystallization in closed platinum crucibles under an air atmosphere. The starting materials consisted of reagent grade metal oxide or carbonate powders (99.9% purity), of Na_2CO_3, K_2CO_3, Bi_2O_3 and TiO_2. Stoichiometric amounts were weighed and thoroughly mixed. The ground powders were then calcined in closed platinum crucibles for 12 hours at 800 °C in air, re-ground and calcined again under identical conditions. Powder samples were then obtained by grinding as-grown crystals. Phase characterization and composition were confirmed using x-ray diffraction and microprobe analysis.

X-ray powder diffraction data on NKBT were recorded with a Stoe STADI 2P automatic powder diffractometer working in transmission mode and fitted with a curved position-sensitive detector. Each NKBT powder was scanned through a 2θ-range of 20–80° with a step size of

0.01° using Cu Kα radiation. The lattice parameters were calculated using Si as internal standard.

Raman spectra of NKBT powders were recorded from 70 to 700 cm^{-1} with a Dilor XY multichannel spectrometer, equipped with a microscope, where the 514.5 nm line of an Ar^+ ion laser was used as excitation line. Experiments were conducted in a micro-Raman backscattering configuration with the laser focused to a 1 μm^2 spot. The instrumental resolution was $2.8 \pm 0.2\ cm^{-1}$. We have verified that laser powers up to 20 mW did not produce significant heating or damage to the sample. Standard experiments were then carried out using incident powers of about 5 mW. Measurements were performed under a $\times 100$ microscope and recorded in a back scattering geometry. In order to characterize the spectral changes in a more qualitative way, we have determined the band positions in the Raman spectra for each substitution rate with the Peakfit software (Jandel).

3. Structure and selection rules

3.1. Crystal structure

The ideal structure of perovskite-type oxides (ABO_3) is essentially simple, with corner-linked anion octahedra, the B cations at the centre of the octahedra and the A cations in the space (co-ordination 12) between the octahedra. Since the discovery of NBT [24] its 300 K crystal structure has been controversial for a long time, rhombohedral [25], triclinic [26] and monoclinic (ICSD-database [27]) structures being considered. Only very recent structure refinements of temperature dependent neutron data of NBT by Jones *et al* [28, 29] could confirm unambiguously the room temperature space group $R3c$. Concerning KBT, authors agree that its room temperature structure is tetragonal [2–4, 30], but the exact space group has not been reported. However, judging from the similar rhombohedral $\rightarrow$ tetragonal $\rightarrow$ cubic phase sequence in NBT [28] and KBT, it is reasonable to suppose it adopts the $P4bm$ space group, as observed for NBT at higher temperatures [31].

Ordering is known to be favoured in B-site substituted perovskites, where there is a substantial charge difference between two cation species. The chemical nature of NBT and KBT raises the question of a possible ordering scheme of the A cations, but, to the best of our knowledge, there has so far been no convincing experimental evidence for this in either NBT or KBT. NKBT is believed to show no ordering scheme either and, thus, broad Raman bands are expected.

3.2. Selection rules and general considerations

The ten atoms in both the rhombohedral NBT and tetragonal KBT unit cells give rise to 27 ($\boldsymbol{k} = \mathbf{0}$) optical modes. These modes can be characterized according to the $3m$ (C_{3v}) and $4mm$ (C_{4v}) factor groups of the crystal using group theoretical methods. Although, Raman data on NBT are available in the literature [21–23], up to now the group theoretical analysis of NBT has been restricted to cubic $Fm\bar{3}m$ and $Pm\bar{3}m$ space groups [21, 22, 32] or to qualitative considerations [23]. For KBT neither Raman spectra nor selection rules have been reported. Therefore, we decided to undertake a detailed analysis using the correlation method, as reviewed by Fateley *et al* [33].

The group theory treatment leads for NBT, using rhombohedral axes, to 13 Raman-active modes

$$\Gamma_{Raman,NBT} = 7A_1 + 6E$$

Table 1. Irreducible representations for (a) NBT and (b) KBT determined by the correlation method. Crystal structure details, correlation used and site representations are also given.

(a) NBT, space group $R3c$ (C_{3v}^6)

Atom	Site [a]	[b]	Site representation	$3m$ C_{3v} factor group representation A_1	A_2	E
Na/Bi	2a	3 (C_3)	2A + 2E	1	1	2
Ti	2a	3 (C_3)	2A + 2E	1	1	2
O	6b	1 (C_1)	18A	6	6	3
			Γ	8	8	7
			$\Gamma_{acoust.}$	1		1
			$\Gamma_{opt.}$	7	8	6
			$\Gamma_{Raman/IR}$	7		6
			Γ_{silent}		8	

[a] Site occupied, Wyckoff notation.
[b] Site symmetry, Schoenflies symbol.

(b) KBT, space group $P4bm$ (C_{4v}^2)

Atom	Site [a]	[b]	[c]	Site representation	$4mm$ C_{4v} factor group representation A_1	A_2	B_1	B_2	E
Na/Bi	2b	$mm2$ (C_{2v})	σ^d	$2A_1 + 2B_1 + 2B_2$	1			1	2
Ti	2a	4 (C_4)		2A + 2E	1	1			2
O	2a	4 (C_4)		2A + 2E	1	1			2
O	4c	m (C_s)	σ^d	$8A' + 4A''$	1	3	3	1	2
				Γ	4	5	3	2	8
				$\Gamma_{acoust.}$	1				1
				$\Gamma_{opt.}$	3	5	3	2	7
				Γ_{Raman}	3		3	2	7
				Γ_{IR}	3				7
				Γ_{silent}		5			

[a] Site occupied, Wyckoff notation.
[b] Site symmetry, Schoenflies symbol.
[c] Site elements used for the correlation between the site group and the factor group.

while the tetragonal KBT structure gives 15 Raman-active modes

$$\Gamma_{Raman,KBT} = 3A_1 + 3B_1 + 2B_2 + 7E.$$

One A_1 and one doubly degenerate E mode correspond for both materials to acoustic modes. Table 1 presents a detailed overview of the symmetry and activity of the different modes in NBT and KBT. In principle, from a group theoretical point of view, NBT and KBT single crystals should be easily distinguished in a polarized Raman study, since the distribution of Raman active vibrational modes into different representations is different. This distinction is not straightforward for powder samples. However, the disorder on the A sites could not only lead to broad bands (making it difficult to distinguish different modes), but also to a breakdown of the selection rules, as has been observed for other perovskites. Moreover, some Raman modes for NBT and KBT are also IR active and thus their frequency depends on their longitudinal (LO) or transverse (TO) character, leading to a broadening of the bands in the

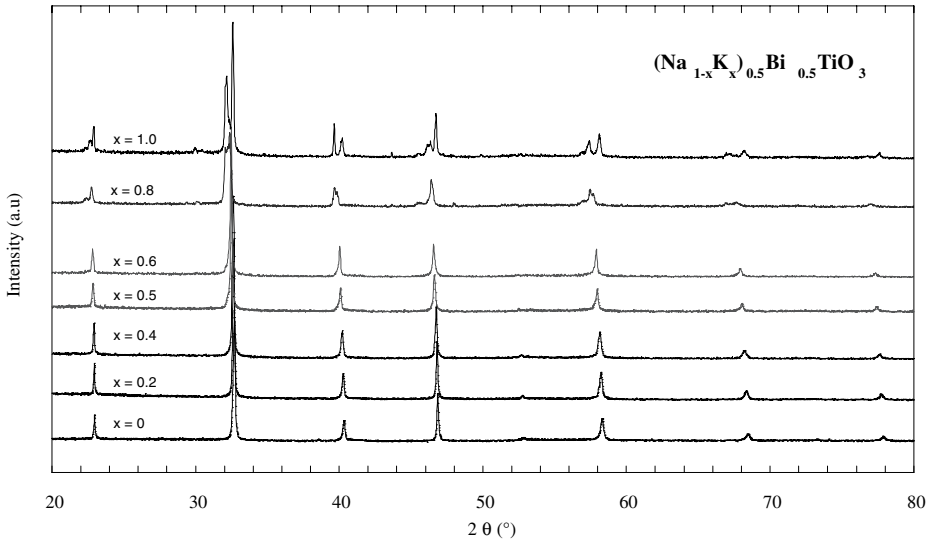

Figure 2. X-ray powder diffraction pattern for $Na_{0.5-x}K_xBi_{0.5}TiO_3$.

polycrystalline samples. Therefore, it is useful to discuss also the expected spectral changes in a more qualitative manner.

The atomic mass of sodium ($m_{Na} = 22.99$) and potassium ($m_K = 39.10$) are, when compared with the heavy bismuth cation ($m_{Bi} = 208.98$), similar and thus a mass effect should be considered to be negligible for most of the modes, except for those involving mainly these cations. On the other hand their ionic radii are quite different, $r_{Na^+} = 1.02$ Å compared with $r_{K^+} = 1.33$ Å. The increase of the ionic radii, when going from Na^+ to K^+, leads naturally to a distortion of the structural framework, and polyhedron distortion in oxides is known to result in a high-frequency shift [34–37]. Any change in the crystal structure or physical properties will, in principle, lead to a variation in the phonon behaviour, and the analysis of the frequency, intensity and linewidth evolution of the whole spectra as a function of the substitution rate is expected to give insight into the change of phase. Such an analysis is known as hard mode spectroscopy [15, 38–40], in contrast to the analysis of directly involved soft modes, and has been shown to be a powerful method for the analysis of phase changes.

4. Results and discussion

4.1. X-ray diffraction

It is known that the location of a phase boundary depends upon the degree of lattice distortion of the end-members of the solid solution [1]. Considering the small tetragonal lattice distortion of KBT ($c/a \approx 1.02$) it might be expected that for small K^+ concentrations NKBT maintains the NBT rhombohedral structure. On the other hand, the ionic radius of the K^+ ($r_{K^+} = 1.33$ Å) is considerably larger than that of Na^+ ($r_{Na^+} = 1.02$ Å). Previous published works on NKBT reported a room-temperature phase boundary for x close to 0.2 [2–4].

As shown in figure 2, our powder XRD results do not show a significant change for $x < 0.8$. For instance, as shown in the scan of a small 2θ-region (figure 3), the split of the {200} reflection is obvious for $x = 0.8$, thus indicating tetragonal symmetry. Generally, the occurrence of a split reflection alone does not constitute sufficient evidence, because a very

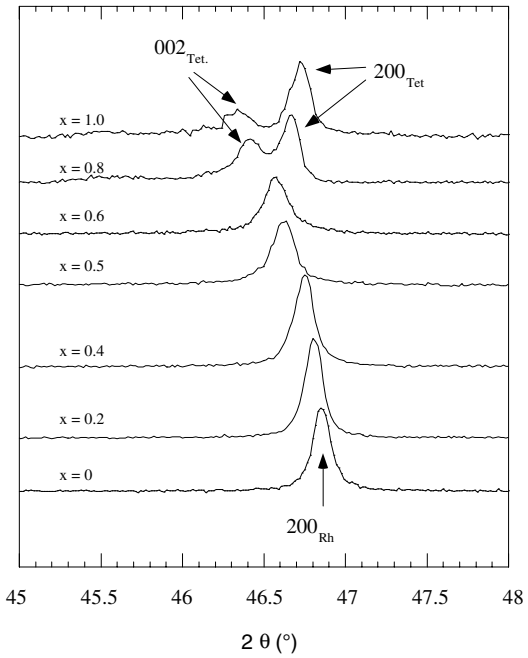

Figure 3. Detailed scan of x-ray reflections for $(Na_{1-x}K_x)_{0.5}Bi_{0.5}TiO_3$ in the 45–48° 2θ-region.

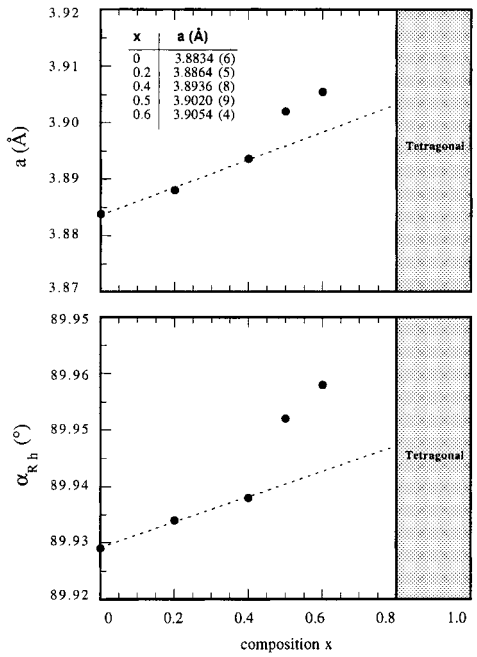

Figure 4. Evolution of the lattice parameters a and the rhombohedral lattice distortion α for $(Na_{1-x}K_x)_{0.5}Bi_{0.5}TiO_3$ ($x \leqslant 0.8$) under the assumption of an $R3c$ space group. The refined values of the lattice constants and standard deviations are also given.

slight lattice distortion would not result in a resolvable splitting. However, the change in diffraction pattern between x of 0.6 and 0.8 is so large that a crystal structural change in this region is strongly suggested.

It is also interesting to examine more precisely the results obtained for the $0 \leqslant x \leqslant 0.6$ range. When a rhombohedral lattice is considered for $x < 0.8$ and the lattice parameters and rhombohedral lattice distorsions are plotted against x (figure 4) it can be seen that the slope changes for $x \approx 0.4$–0.5, which might indicate a second structural change. For comparison, the tetragonal lattice constants for $x = 0.8$ are $a = 3.9134(7)$ Å and $c = 3.9715(8)$ Å and for $x = 1$, $a = 3.9360(1)$ Å and $c = 3.9884(1)$ Å.

It is worth comparing our data with literature results, knowing that a rhombohedral/tetragonal two-phase-region for $0.18 \leqslant x \leqslant 0.6$ [3] or a pseudo-cubic phase for $0.17 \leqslant x \leqslant 0.4$ [2] have been reported. Our x-ray diffraction patterns give no evidence for a coexistence of rhombohedral and tetragonal phases; the results reported by Elkechai *et al* [3] are most likely to result from different preparation conditions. On the other hand, mainly because of the instrumental resolution, we cannot exclude the presence of another pseudo-cubic phase.

4.2. Raman spectroscopy

4.2.1. NBT and KBT reference spectra. Before discussing the phonon characteristics of the NKBT solid solution it is important to have reference data for the end members. Figure 5 shows room-temperature Raman spectra of NBT and KBT, together with their spectral deconvolution into Lorentzian-shape peaks.

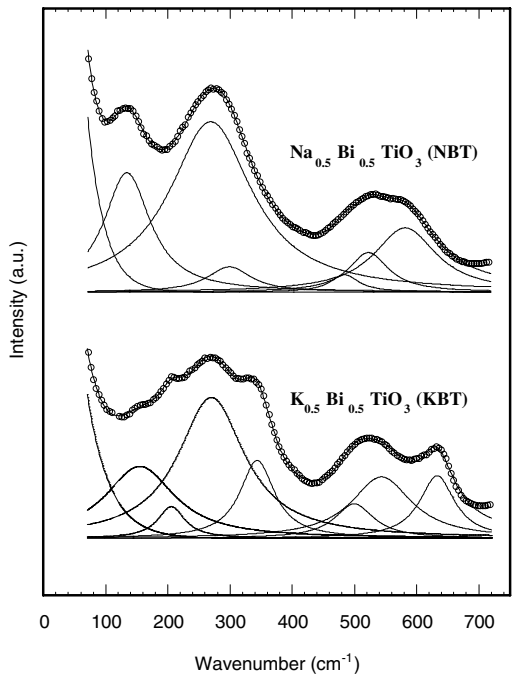

Figure 5. Room temperature Raman spectra of $Na_{0.5}Bi_{0.5}TiO_3$ (NBT) and $K_{0.5}Bi_{0.5}TiO_3$ (KBT). The open circles are plotted for every fifth point of the experimental data and the solid lines display the spectral deconvolution.

Raman bands for NBT and KBT are relatively broad, which is mainly due to the disorder on the A site, but results also from overlapping Raman modes. The Raman spectrum observed for NBT is similar to already reported data [21–23]. However, we deconvolute the 100 to 700 cm^{-1} range into six peaks, while in earlier studies this range has been discussed only on the basis of three bands [22, 23]. To some extent the broad band at $\approx$260 cm^{-1} can be fitted as a single line, but the introduction of an underlying component on the high frequency side leads to a better overall fit. Attempts to use three peaks for the broad feature at 200 to 300 cm^{-1} and four peaks for the one at 480 to 600 cm^{-1} in NBT failed.

As expected from the crystal structure, the KBT Raman spectrum shows a different spectral fingerprint compared with NBT. Its spectrum has been deconvoluted into seven peaks in the 100 to 700 cm^{-1} range, reflecting the higher number of bands according to the group theory results in section 3.2. As a consequence of the difference between NBT and KBT Raman spectra we should be able to follow the evolution of the phonon behaviour in the NKBT solid solution.

4.2.2. NKBT solid solution. Representative powder Raman spectra of NKBT ($x = 0$, 0.2, 0.4, 0.5, 0.6, 0.8 and 1.0), recorded at room temperature, are shown in figure 6. Several qualitative features in the NKBT Raman spectra can be discerned for increasing K^+ content:

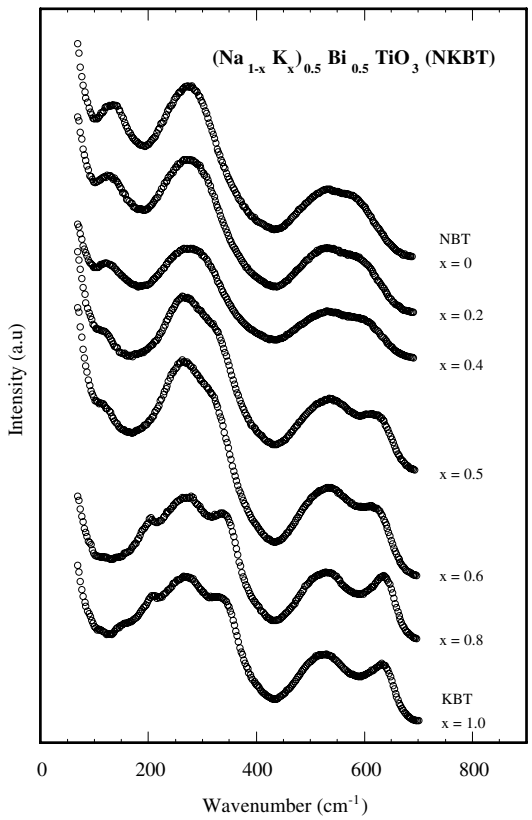

Figure 6. Room temperature Raman spectra for $(Na_{1-x}K_x)_{0.5}Bi_{0.5}TiO_3$. The shifts and splitting of the phonon bands are due to structural phase transitions between the end members $Na_{0.5}Bi_{0.5}TiO_3$ (NBT) and $K_{0.5}Bi_{0.5}TiO_3$ (KBT).

(i) Except for some peaks, especially that at about 135 cm^{-1}, there is a general upward shift of the Raman frequencies.
(ii) The broad band centred around 260 cm^{-1} is first split into two and then into three components.
(iii) The overlapping bands at 400–650 cm^{-1} are split.

In the following, these three points will be separately discussed as hard-mode features.

(i) *135 cm^{-1} band.* As mentioned above, the 135 cm^{-1} peak (earlier assigned to A_1 symmetry [23]) is the only band showing a clear low frequency shift. However, the frequency change is still relatively weak (14 cm^{-1} for $x = 0.40$) and cannot be interpreted as a directly involved soft mode. Since the band position changes with substitution rate, this band should be assigned to vibrations involving the A site, because vibrations involving the B site are expected to be unaffected by the substitution. Low frequency A_1 modes are known to be dominated by cation displacement along a crystallographic axis and, as a consequence, the downward shift should be mainly attributed to the increasing mass on the A site.
In the harmonic oscillator approximation with negligible force constant changes, the masses and frequencies are related by the following equation.

$$(\nu_{x=0}/\nu_{x=0.4})^2 \approx (M_{x=0.4})/(M_{x=0}) \qquad \text{where } \nu_{x=0}/\nu_{x=0.4} \approx 1.11.$$

The main difficulty in a study of the mass effect is the knowledge of the masses and the vibrational picture to be taken into consideration, with the difficulty in our case that three different species (K^+/Na^+ and Bi^{3+}) are present on the A site. Two situations are useful to consider:

(a) *The 'virtual ion' model [41], where the 'virtual ion' can be seen as an ion with the average properties of the cations on the A site.* Generally, the 'virtual ion' concept is a good approximation when mass and force constant differences are small. This is not the case for NBT, since the mass of the Bi cation is nearly ten times that of the Na cation and it is expected to vibrate at significantly lower frequencies than the Na cation. Furthermore, the Na–O and Bi–O bonding (and therefore the force constants) are not expected to be similar, as a result of the particular behaviour of the stereo-active lone pair of Bi^{3+} [28, 31, 42]. Furthermore, in the virtual ion model, the shift of the 135 cm^{-1} band for $x = 0.4$ would be very small ($\approx$3 cm^{-1}), while 14 cm^{-1} was observed experimentally. As consequence, the virtual ion model is unlikely to represent the physical reality.
(b) *Two (or more) mode behaviour (as exemplified by $Si_{1-x}Ge_x$ [43]).* Here the compound may be viewed as an alternation of zones richer in one constituent than the other, these zones being of nanometre size, in such a way that diffraction cannot reveal a phase separation. For NBT this would lead to separated Bi–O and Na–O bands. In NKBT, with Na and K having a similar mass, the latter band is expected to become an Na_{1-x}/K_x band, shifting progressively according to the virtual ion model. In fact, the experimental value of $\nu_{x=0}/\nu_{x=0.4} \approx 1.11$ corresponds well with $((0.6{*}m_{Na} + 0.4{*}m_K)/m_{Na})^{1/2} \approx 1.12$. This supports the scenario of a two-mode behaviour for NBT, where one of the bands shifts for NKBT with the substitution rate to lower frequency according to the virtual ion model. Unfortunately, our Raman spectra do not allow us to observe the Bi–O band, which is expected to be located at very low frequency because of the important Bi mass, as has been observed for α-Bi_2O_3 [44]. Assuming that the 135 cm^{-1} band is an Na/K–O band, its presence implies that nanometer-size domains exist, because otherwise the phonon lifetime would have been too short to result in a defined Raman peak. Such nanodomains should be

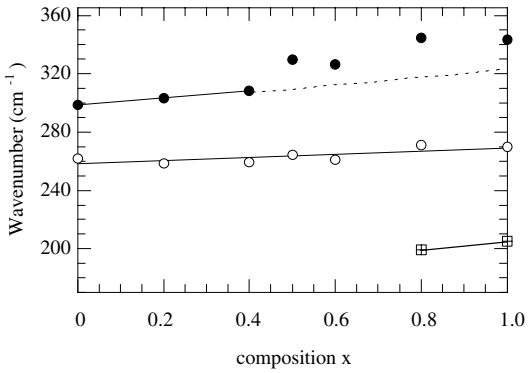

Figure 7. Band position change in the Raman spectra of $(Na_{1-x}K_x)_{0.5}Bi_{0.5}TiO_3$ as a function of composition for the broad feature at 200 to 300 cm^{-1}. The lines are guides for the eyes to emphasize spectral changes.

seen as local $Bi^{3+}TiO_3$ and $(Na_{1-x}K_x)^{+}TiO_3$ clusters or even one-dimensional chains (but no superstructure).

In principle such domains are undetectable by x-ray diffraction with its coherence length of ≈20 unit cells. However, the presence of diffuse scattering in NKBT crystals could support the scenario. X-ray diffuse scattering and x-ray topography studies are currently in progress and early results support the occurrence of local $Bi^{3+}TiO_3$ and $(Na_{1-x}K_x)^{+}TiO_3$ arrangements. Furthermore, transmission electron microscopy (TEM) is an efficient probe for the study of local structure on an atomic level. A preliminary TEM investigation of pure NBT suggests the existence of local one-dimensional $Bi^{3+}TiO_3$ and $Na^{+}TiO_3$ chains over several unit cells.

(ii) *200 to 300 cm^{-1} region*. In this frequency region the most obvious spectral changes are observed for the NKBT solid solution. Figure 7 presents the evolution in frequency for the bands occurring in this region.

The first obvious change for the broad feature is observed for $x = 0.5$, where the underlying component appears as a clear shoulder on the high frequency side of the 280 cm^{-1} peak, departing from the linear evolution given for lower substitution rates (figure 7). This appearance of the shoulder might be seen as the rise of an underlying component, but the gradient change in frequency is more likely to be interpreted as a structural change.

The second, more pronounced spectral change occurs for $x = 0.8$. In fact, the sudden appearance of the peak at ≈200 cm^{-1} can be seen as the most sensitive indication in the NKBT Raman spectra for the presence of the tetragonal KBT phase and thus a structural change. In general, it is one of the advantages of Raman spectroscopy, over diffraction methods, that phonon signals from local parts of a sample are simply superimposed so that the macroscopically measured spectrum contains all local information. In fact, Raman spectroscopy is sensitive even to very small phase fractions, and the simple fact that the peak at ≈200 cm^{-1} has not been observed for lower substitution rates allows us to rule out a tetragonal–rhombohedral two-phase region, which is in contrast to results reported in [3]. Finally, it can be seen that the dominant peak of the broad feature at ≈280 cm^{-1} roughly maintains its frequency position. This observation, together with the fact that a strong peak at essentially the same position has been observed in the Raman spectra of tetragonal $BaTiO_3$ and $PbTiO_3$, is an indication that this band must be dominated by Ti–O vibrations.

(iii) *400 to 700 cm^{-1} region*. The 400 to 700 cm^{-1} region is composed of three bands, two

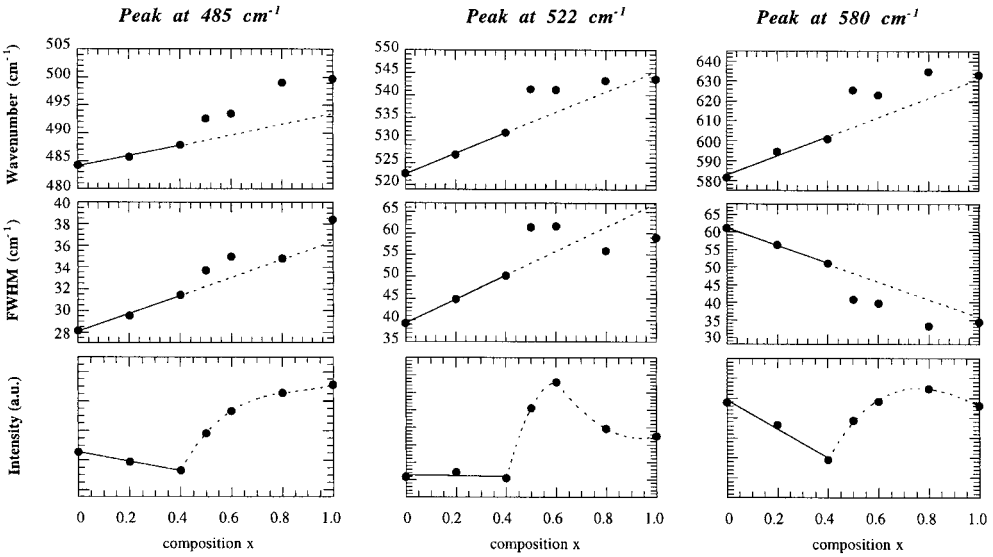

Figure 8. Band position, FWHM and intensity change in the Raman spectra of $(Na_{1-x}K_x)_{0.5}Bi_{0.5}TiO_3$ as a function of composition for the broad feature at 450 to 650 cm^{-1}. The lines are guides for the eyes to emphasize spectral changes.

dominating and one underlying band. Since this region does not show drastic spectral changes like the one at 200 to 300 cm^{-1}, it is useful to plot the substitution dependent evolution of the frequency, the FWHM and the intensity for each of the three lines (figure 8). According to the concept of hard mode spectroscopy [15, 38–40], these three bands should be sensitive towards structural changes. However, 'hard mode features' are slight and generally more or less pronounced depending on the particular phonon. The latter point can be easily verified in figure 8, showing that spectral changes are clearly visible for some graphs, while they are less pronounced in others. The overall feature in figure 8, most visible in the intensity, is that the phonon characteristics in NKBT show a pronounced change between $x = 0.4$ and $x = 0.5$, which is evidence of a phase change and, therefore, strengthens the interpretation above for the high frequency part of the 200–300 cm^{-1} region.

It is interesting to examine the 400 to 600 cm^{-1} region with regard to a second change at $x = 0.8$, marked by the above sudden appearance of a phonon at $\approx$200 cm^{-1}. In fact, for some of the peak characteristics, a change in the phonon behaviour can be observed between $x = 0.6$ and $x = 0.8$; this is especially the case for the intensity and FWHM of the 522 cm^{-1} band and to a slighter extent for others like the wavenumber shift observed for the 485 and 580 cm^{-1} bands. However, the latter observations are based only on a limited number of experimental points and further Raman studies using intermediate substitution rates in the $0.4 < x < 0.8$ range are needed.

It remains to discuss the high frequency shift. For oxides it is known that high frequency Raman bands are dominated by vibrations involving mainly oxygen displacements and, therefore, are expected to be unaffected by the mass of the cation. However, the chemical nature of the cation can influence the frequency of these bands by the other determining element of a harmonic oscillator, the force constants (i.e. bonding, repulsion effects etc). Based on the arguments in section 3.2 this shift should be interpreted as resulting from the increasing average ionic radii on the A site for an increasing K^+ substitution rate. In

order to support this argument for titanate perovskites, note that the Raman frequencies in $BaTiO_3$ are higher than in $PbTiO_3$ ($r_{Ba^{2+}} > r_{Pb^{2+}}$).

5. Phase transition mechanism

The first transition at $x = 0.40$ is clearly demonstrated by Raman spectroscopy and to a smaller extent by x-ray diffraction, while the second transition is mainly suggested by x-ray diffraction and supported by Raman spectroscopy. It is the complementary use of x-ray diffraction and Raman spectroscopy which allows us to provide evidence for both of them. While the phase on the NBT side is rhombohedral and the phase on the KBT side is tetragonal, the structure of the intermediate phase is unknown. The occurrence of an intermediate phase, in itself, is not surprising. It has already been pointed out [45] that the structural change from an $R3c$ to a $P4bm$ space group is very large (not being in a pure super- or sub-group relation) while an intermediate phase could make such a change energetically more plausible. From a symmetric or group theoretical point of view two intermediate structures might be considered for NKBT:

(i) The cubic phase $Pm\bar{3}m$, being the super-group of $R3c$ ($R3c \rightarrow R\bar{3}c \rightarrow Pm\bar{3}m$) and $P4bm$ ($P4bm \rightarrow P4/mbm \rightarrow P4/mmm \rightarrow Pm\bar{3}m$).
(ii) The monoclinic phase Cc, being a sub-group of $R3c$ ($Cc \rightarrow R3c$) and $P4bm$($Cc \rightarrow Cm \rightarrow Cmm2 \rightarrow P4bm$).

Similar mechanisms for other perovskites have been discussed recently for NBT [45], $PbZr_{0.52}Ti_{0.48}O_3$ (PZT) [46, 47], $PbFe_{0.5}Nb_{0.5}O_3$ [48] and $Pb(Sc_{0.5}Ta_{0.5})O_3$ [16]. For the temperature-induced rhombohedral → tetragonal SPT in NBT an intermediate cubic $Pm\bar{3}m$ phase or an amorphous phase has been suggested based on birefringence measurements [45]. On the basis of our Raman spectra we should rule out a cubic intermediate phase, since first-order Raman modes are not allowed in the $Pm\bar{3}m$ space group.

Noheda *et al* [46, 47] reported a synchrotron x-ray diffraction experiment on $PbZr_{0.52}Ti_{0.48}O_3$ giving evidence for a monoclinic phase, which provides a 'bridge' between tetragonal and rhombohedral regions. This new feature suggests a 'morphotropic phase' rather than a morphotropic phase boundary. For the NKBT solid solution the experimental resolution of our x-ray diffractometer does not allow us to decide whether a monoclinic phase is present or not. On the other hand, from a Raman spectroscopy point of view, the Cc space group is unlikely, because 27 modes would be Raman active and such an increase in number of bands has not been observed.

According to Bismayer *et al* [16] the different steps in a cascade of phase transitions involving a symmetry change should also be considered. Inspecting the different steps given above, Cm and $Cmm2$ and $R\bar{3}c$ can be ruled out by using similar arguments as for Cc. The space groups $P4/mbm$ and $P4/mmm$ would lead to a slightly lower number of bands (for instance ten for $P4/mbm$), which has not been observed. In our opinion no further judgment about the intermediate phase is reasonable on the basis of our data and further structural work is needed.

6. Conclusion

We have described a study of the structural phase transitions for the $Na_{0.5-x}K_xBi_{0.5}TiO_3$ solid solution using x-ray diffraction and Raman spectroscopy. The phonon characteristics of NKBT have been analysed by using the concept of hard mode spectroscopy allowing the elucidation of small spectral changes related to phase transitions of NKBT. All bands show

a high frequency shift with increasing substitution rate. The only exception is the band at 135 cm^{-1}, being assigned to an Na/K–O vibration, which suggests the existence of nanosized $Bi^{3+}TiO_3$ and $(Na_{1-x}K_x)^{+}TiO_3$ clusters. It is the complementary use of x-ray diffraction and Raman spectroscopy on NKBT that has allowed us to propose the existence of an intermediate phase for x between $\approx$0.5 and 0.8, which might be seen as a bridge phase 'buffering' the important rhombohedral–tetragonal symmetry change from NBT to KBT. Further diffraction and spectroscopic work is necessary in order to determine the exact localization of the SPT and the structure of the intermediate phase. We have shown that Raman spectroscopy is a good candidate for this kind of study in NKBT and we encourage the study of physical properties of the intermediate phase which might lead to a new lead-free ferroelectric relaxor with interesting electromechanical properties.

Acknowledgments

The authors are grateful to the Engineering and Physical Science Research Council for a grant that enabled this work to be pursued and to K Roleder and M Geday for helpful discussions on NBT.

References

[1] Jaffe B, Cook W R and Jaffe H 1971 *Piezoelectric Ceramics* (London: Academic)
[2] Pronin I P, Parfenova N N, Zaitseva N V, Isupov V A and Smolenskii G A 1982 *Sov. Phys.–Solid State* **24** 1060–2
[3] Elkechai O, Manier M and Mercurio J P 1996 *Phys. Status Solidi* a **157** 499–506
[4] Yamada Y, Akutsu T, Asada H, Nozawa K, Hachachiga S, Kurosaki T, Fujiki H, Hozumi K, Kawamura T, Amakawa T, Hirota K and Ikeda T 1995 *Japan. J. Appl. Phys.* **34** 5462–6
[5] Hong K S and Park S E 1996 *J. Appl. Phys.* **79** 388–92
[6] Park S E and Hong K S 1996 *J. Appl. Phys.* **79** 383–7
[7] Isupov V A, Strelets P L, Serova I A, Yataenko N D and Shirobokikh T M 1964 *Sov. Phys.–Solid State* **6** 615–19
[8] Sakata K, Takenaka T and Naitou Y 1992 *Ferroelectrics* **131** 219–26
[9] Elkechai O, Marchet P, Thomas P, Manier M and Mercurio J-P 1997 *J. Mater. Chem.* **7** 91–7
[10] Park S E and Hong K S 1997 *J. Mater. Res.* **12** 2152–7
[11] Sakata K and Masuda Y 1974 *Ferroelectrics* **7** 347–9
[12] Emelyanov S M, Raevskii I P and Prokopalo O I 1983 *Sov. Phys.–Solid State* **25** 889–91
[13] Siny I G, Tu C S and Schmidt V H 1995 *Phys. Rev.* B **51** 5659–64
[14] Tu C S, Siny I G and Schmidt V H 1994 *Phys. Rev.* B **49** 11 550–9
[15] Salje E K H and Bismayer U 1997 *Phase Transitions* **63** 1–75
[16] Bismayer U, Devarajan V and Groves P 1989 *J. Phys.: Condens. Matter* **1** 6977–86
[17] Frantti J, Lantto V and Lapplalainen J 1996 *J. Appl. Phys.* **79** 1065–72
[18] Frantti J and Lanatto V 1997 *Phys. Rev.* B **56** 221–36
[19] Zhang H, Leppävuori S and Karjalainen P 1995 *J. Appl. Phys.* **77** 2691–6
[20] Meng J, Zou G, Ma Y, Wang X and Zhao M 1994 *J. Phys.: Condens. Matter* **6** 6549–56
[21] Siny I G, Smirnova T A and Kruzina T V 1991 *Ferroelectrics* **124** 207–12
[22] Siny I G, Smirnova T A and Kruzina T V 1991 *Sov. Phys.–Solid State* **33** 61–4
[23] Zhang M S and Scott J F 1986 *Ferroelectr. Lett.* **6** 147–52
[24] Smolenskii G A, Isupov V A, Agranovskaya A I and Krainik N N 1960 *Sov. Phys.–Solid State* **2** 2982–5
[25] Suchanicz J and Kwapulinski J 1995 *Ferroelectrics* **165** 249–53
[26] Isupov V A, Pronin I P and Kruzina T V 1984 *Ferroelectr. Lett.* **2** 205–8
[27] Zhou F, Xu Y Y, Li D Y, He C F and Gao M 1989 *Powder Diffraction* **4** 223–6
[28] Jones G O and Thomas P A 1999 *Acta Crystallogr.* C *Suppl.* A **55** 493–4
[29] Jones G A and Thomas P A 2000 *Acta Crystallogr.* at press
[30] Ivanova V V, Kapyshev A G, Venevtsev Y and Zhdanov G S 1962 *Izv. Akad. Nauk. SSSR Ser. Fiz.* **26** 354–6
[31] Jones G A and Thomas P A 2000 *Acta Crystallogr.* B submitted
[32] Siny I G, Katiyar R S and Bhalla A S 1998 *J. Raman Spectrosc.* **29** 385–90
[33] Fateley W G, Devitt N T M and Bentley F F 1971 *Appl. Spectrosc.* **25** 155–73

[34] Kreisel J, Lucazeau G and Vincent H 1998 *J. Solid State Chem.* **137** 127–37
[35] Kreisel J, Vincent H and Lucazeau G 1999 *J. Raman Spectrosc.* **30** 115–20
[36] Tarte P 1967 *Spectrochim. Acta* A **23** 2127–37
[37] Tarte P, Rulmont A, Liégeois-Duycckaerts M, Cahay R and Winand J M 1990 *Solid State Ion.* **42** 177–96
[38] Petzelt J and Dvorak V 1976 *J. Phys. C: Solid State Phys.* **9** 1587–601
[39] Petzelt J and Dvorak V 1976 *J. Phys. C: Solid State Phys.* **9** 1571–86
[40] Bismayer U 1990 *Phase Transitions* **27** 211–67
[41] Barker A S and Sievers A J 1975 *Rev. Mod. Phys.* **47** S1–37
[42] Park J H, Woodward P M, Parise J B, Reeder R J, Lubomirsky I and Stafsudd O 1999 *Chem. Mater.* **11** 177–83
[43] Alonso M I and Winer K 1989 *Phys. Rev.* B **39** 10 056–62
[44] Denisov V N, Ivlev A N, Lipin A S, Mavrin B N and Orlov V G 1997 *J. Phys.: Condens. Matter* **9** 4967–78
[45] Geday M, Kreisel J, Roleder K and Glazer A M 2000 *J. Appl. Crystallogr.* at press
[46] Noheda B, Cox D E, Shirane G, Gonzalo J A, Cross L E and Park S E 1999 *Appl. Phys. Lett.* **74** 2059–61
[47] Noheda B, Gonzalo J A, Cross L E, Guo R, Park S E, Cox D E and Shirane G 2000 *Phys. Rev.* B at press
[48] Bonny V, Bonin M, Sciau P, Schenk K J and Chapius G 1997 *Solid State Commun.* **102** 347–52